Journal of Mammalian Evolution
https://doi.org/10.1007/s10914-021-09593-2

ORIGINAL PAPER

Morphological and Functional Divergence of the Lower Jaw Between Native and Invasive Red Foxes

Colline Brassard[1] · Jesse L. Forbes-Harper[2] · Heather M. Crawford[2] · John-Michael Stuart[2] · Natalie M. Warburton[2] · Michael C. Calver[2] · Peter Adams[2] · Elodie Monchâtre-Leroy[3] · Jacques Barrat[3] · Sandrine Lesellier[3] · Claude Guintard[4,5] · Hélène Garès[6] · Arnaud Larralle[7] · Raymond Triquet[8] · Marilaine Merlin[1] · Raphaël Cornette[9] · Anthony Herrel[1] · Patricia A. Fleming[2]

Accepted: 30 November 2021

Abstract

The introduction of European red foxes in Australia in the late mid-nineteenth century has resulted in the spread of this invasive species across the continent. The morphological and functional divergence of this relatively recently introduced population has not been explored to date, yet it may provide unique insights into adaptability of this widespread carnivore to very different environments. Here we used three-dimensional geometric morphometric approaches and dissections to explore differences in mandible form and function between two populations: one from France and the other from Western Australia. Bite force was predicted for Australian foxes using partial least squares (PLS) regression models based on the observed covariation between estimated bite force (from muscle dissections) and mandible form in French foxes. Muscle contributions were estimated based on Euclidean distances between landmarks that provide insights into muscle lever arms. Despite the greater sample size, Australian foxes show reduced variability in mandible shape compared with French foxes. The mandibles of adult French foxes tend to be slightly smaller and they also strongly differ in shape from the Australian foxes in functionally important areas of the mandible such as muscle insertion areas. This is accompanied by significant differences in the predicted bite force, even relative to size, and muscle contribution: the bite of Australian foxes is weaker and they show greater use of their temporalis muscle compared to French foxes. The reduced variability suggests a founder effect or stabilizing selection on a specific morphology, which was supported by statistical tests. The corresponding anatomical traits suggest different functional demands likely due to differences in diet or competition. Future studies investigating the drivers of variation in mandible shape in native and invasive populations, including data from the original source of the Australian introductions, are needed to better understand the observed differences.

Keywords *Vulpes vulpes* · Mandible · Shape · Geometric morphometrics · Biological invasions

✉ Colline Brassard
co.brassard@gmail.com

[1] UMR 7179 Mécanismes Adaptatifs et Evolution (CNRS, MNHN), Muséum national d'Histoire naturelle, Paris, France

[2] Environmental and Conservation Sciences, Harry Butler Research Centre, Murdoch University, Murdoch, WA, Australia

[3] ANSES, Laboratoire de la rage et de la faune sauvage, Station expérimentale d'Atton, Malzéville, France

[4] Laboratoire d'Anatomie comparée, Ecole Nationale Vétérinaire, de l'Agroalimentaire et de l'Alimentation, Nantes Atlantique – ONIRIS, Nantes Cedex 03, France

[5] GEROM, UPRES EA 4658, LABCOM ANR NEXTBONE, Faculté de santé de l'Université d'Angers, Angers, France

[6] Direction des Services Vétérinaires – D.D.C.S.P.P. de la Dordogne, Périgueux, France

[7] 24210 Brouchaud, France

[8] Université de Lille III, Villeneuve d'Ascq, France

[9] UMR 7205 Institut de Systématique, Evolution, Biodiversité (CNRS, MNHN, UPMC, EPHE), Muséum national d'Histoire naturelle, Paris, France

Published online: 17 January 2022

Introduction

The red fox *Vulpes vulpes* is one of the most widespread mammalian carnivore species on the planet (Schipper et al. 2008). Native across the entire Holarctic, the European red fox was successfully introduced into southeast Australia in the middle of the nineteenth century for recreational hunting (Rolls 1969; Cox 2004; Saunders et al. 2010; Abbott 2011). Some of the first foxes introduced were sourced from France and sold in the London markets (Abbott 2011). Foxes arrived on the opposite side of the continent (Western Australia) by 1906. With the exception of tropical areas in the north and some off-shore islands, foxes have spread across the continent and are today invasive and abundant (Forsyth 2004; Statham et al. 2014; Hradsky et al. 2017), with more than 7.2 million foxes estimated across the continent in 2012 (Lewis-Stempel 2020). This widely distributed and highly adaptable species thus provides a unique opportunity to investigate divergence between native and invasive populations.

Previous studies have documented founder effects and genetic drift in Australian red foxes although limited loss of alleles by genetic drift appears to have occurred (Lade et al. 1996). Surprisingly, the morphology of red foxes has never been compared between native European and invasive Australian populations. Given that the population of the Australian red foxes was established by a very small number of European red foxes, their morphology likely had a disproportionate impact on the variation observed in the invasive population (Allendorf and Lundquist 2003), which may result in a relatively lower disparity in morphology relative to native populations of red foxes.

Geographical variation (between continents or regions) in the morphology of red foxes has been previously reported (Churcher 1959; Huson and Page 1980; Szuma 2008; Sacks et al. 2010; Jojić et al. 2017; Stepkovitch et al. 2019). For example, Szuma (2008) demonstrated on a vast sample of 3806 red foxes skulls that tooth size varies depending on geo-climatic factors, following Bergmann's rule. Churcher (1959) found differences in dental and cranial measurements between North American and Eurasian red foxes. Huson and Page (1980) identified variation in skull measurements between six counties in Wales, probably in response to adaptations to local environmental conditions (the authors do not entirely explore these, yet they suppose differences between some locations may be related to differences in altitude, which correlates with differences in rainfall that may affect the diet of the foxes). Jojić et al. (2017) used geometric morphometric techniques and found that cranial shape of Serbian red foxes varies geographically. These differences have been suggested to be the result of local adaptation (Sacks et al. 2010; Edwards et al. 2012), genetic drift, or plastic morphological changes in response to different environmental conditions (West-Eberhard 1989).

The mandible and the masticatory muscles are particularly of interest to explore the morphological divergence between native and invasive populations, as they directly impact bite force (Brassard et al. 2021), which is a major indicator of diet in vertebrates (e.g., Christiansen and Wroe 2007; Nogueira et al. 2009), including carnivores (Christiansen and Wroe 2007). Accordingly, differences in mandible shape or muscle volume and/or muscle physiological cross-sectional area (PCSA, a proxy for generated bite force) between native and invasive populations are likely to reflect functional adaptations. As the diet of invasive populations of red foxes in Western Australia (Forbes-Harper et al. 2017) and native populations in Europe (Cavallini and Volpi 1995, 1996) has been documented, this provides baseline data allowing us to interpret potential differences in mandible shape or muscle architecture, in particular in adult foxes (i.e., foxes over 10 months old, as they become sexually mature and growth is expected to be complete; Saunders et al. 1995; Roulichova and Andera 2007).

To date, most bite force estimations in red foxes have been based on the dry-skull method, where the muscle cross-sectional area is approximated from cranial measurements (Forbes-Harper et al. 2017; Magalhães et al. 2020). This two-dimensional method does not include the complex three-dimensional (3D) geometry of the skull, nor muscle architecture per se, in the bite force estimates. Previous studies have suggested that the PCSA of the temporalis muscle tends to be overestimated, whereas that of the masseter and pterygoid muscles tend to be underestimated (Davis et al. 2010). Lever models that take into account the 3D structure of the skull, and PCSA calculated from dissected muscles therefore provided the best predictions of bite force (Davis et al. 2010). The relationships between mandible shape and bite force estimates based on individual muscle data obtained through dissection have been explored in a population of French red foxes (Brassard et al. 2021). The results suggest that bite force predictions are possible using regression models using mandible shape (as 6–7% of variation in mandible shape is explained by variation in estimated bite force, and the strong covariations observed highlighted the particular importance of the mandibular ramus; Brassard et al. 2021). As muscle data are used to build the decision rules of the bite force model, such predictions may provide more accurate estimations than the dry-skull method.

Differences in diet between native and invasive populations may influence the selective pressures acting on the skull through the functional demands placed on bite force. The strong dietary flexibility of European red foxes likely favoured the exploitation of native prey following their introduction to Australia (Fleming et al. 2021). Moreover, the

diet of Australian foxes includes a large proportion of large prey items, either live or as carrion. A review of 85 studies of the diet of the red fox across its distribution within Australia indicated that consumption of large mammal carrion is common, with 13.8 ± 22.4% of individuals yielding livestock remains (range 0–92.6%) and 9.5 ± 13.3% yielding remains of macropodids (range 0–69.1%; Fleming et al. 2021). Some studies carried out in agricultural landscapes report much higher values. For example, livestock comprised 47–65% of stomach content volume across livestock production areas in Western Australia (Forbes-Harper et al. 2017). Large mammal carrion has also been reported for European studies, with Díaz-Ruiz et al. (2013) reporting carrion present in 15.3 ± 14.2% of the samples across 55 studies of the diet of red foxes from the Iberian Peninsula. Soe et al. (2017) reviewed 66 studies from across 17 European countries (but none from France) and found carrion in 19.2 ± 13.0% of the samples on average. By contrast, domestic mammals (principally sheep and lagomorphs) made up 29% of stomach volume for foxes from western Italy (Cavallini and Volpi 1996). However, large carrion was not reported in the only study of French foxes we found in the literature. Based on a two-year study of fox scats from a park, an agricultural area, and a managed forest in suburban areas in the south of Paris, Castañeda et al. (2020) showed that French foxes instead feed on large to medium-sized birds, hares, small prey (e.g., murid rodents), earthworms, or fruits, with no traces of large mammals in the scat.

Here we used muscle dissections and 3D geometric morphometrics to explore fine-scale morphological and functional differences in the lower jaw of a population of European red foxes from France and invasive red foxes from Western Australia. First, we compared mandible shape and size between the two groups and tested for possible signatures of selection. Next, we compared jaw function. To do so, we developed two predictive models based on the quantitative relationship between muscle data and mandible shape in French foxes (Brassard et al. 2021) to predict the maximal bite force likely to be produced by the Australian foxes. We compared our predictions with previous estimations based on the dry-skull method (Forbes-Harper et al. 2017) as well as estimates based on dissection of the jaw muscles in a sample of Australian foxes. We estimated the relative contribution of each muscle group to bite force based on measurements extracted from landmarks on the mandible that correspond to muscle lever arms. We predicted mandible shape and/or size to be more variable in French (native) foxes compared to Australian (invasive) foxes given the small number of founder animals introduced. We also predicted differences in shape and bite force given the frequent inclusion of large carrion in the diet of invasive foxes (Cavallini and Volpi 1996 *versus* Forbes-Harper et al. 2017) contrary to that of French foxes (Castañeda et al. 2020). Finally, we predicted a more important role for the temporalis muscle in generating bite force for the Australian foxes as this muscle is biomechanically optimised for producing maximum force when the jaws are opened widely (Brassard et al. 2021), likely needed when eating carrion (as carrion remains are large, tough, and consequently chewy).

Material and Methods

Sample and Information

The dataset was composed of the mandibles of 64 French red foxes (with age based on the eruption of the teeth, cranial suture closure, and the porosity of the mandible; Brassard et al. 2021) and 433 red foxes from Western Australia (with age determined through cranial suture closure and counts of canine tooth incremental cementum lines; Forbes-Harper et al. 2017). Most of the foxes were from the southwest Western Australia (Forbes-Harper et al. 2017), with only a few from the Pilbara region in northern Western Australia. As growth is an important factor that may drive variation in mandible size and shape (Brassard et al. 2021) and that is normally complete after one year in red foxes (Roulichova and Andera 2007), we analysed data separately for all foxes ("All") or for "Adults only". Adults represent foxes with a closed basisphenoid-basioccipital suture (Forbes-Harper et al. 2017; Brassard et al. 2021). Accordingly, only 40% of the Australian foxes but 80% of French foxes were classified as adults (Table 1). The others are juveniles or young foxes of less than one year old. Sex is also a factor that may drive variation in mandible shape and size (Forbes-Harper et al. 2017; Brassard et al. 2021). Although sex was not known for a few individuals, the sex ratios were overall homogenous between the samples as confirmed by chi-squared tests performed on the foxes with known sex (Table 1). Detailed information about the samples are reported in Online Resource 1.

Photogrammetry and Geometric Morphometrics

We used photogrammetry to build 3D models of all mandibles. For each mandible, 50 photographs were taken for both the dorsal and ventral side at different angles. The two sides were merged to build a complete model using 'Agisoft PhotoScan' software (© 2014 Agisoft LLC, 27 Gzhatskaya st., St. Petersburg, Russia). The models were cleaned with Geomagic v. 11 (Geomagic, Research Triangle Park, NC, USA) and simplified using Meshlab version 2016.12 (Cignoni et al. 2008).

We used geometric morphometrics to explore the patterns of variation in mandibular shape and size. To do so, 25 homologous anatomical landmarks, 190 sliding

Table 1 Sample sizes of mandibles considered in the analyses of variation between French and Australian red foxes (*Vulpes vulpes*). χ^2 test tests for homogeneity of the sample. BF: estimated bite force from muscle dissections. F: female; M: male; NA: sex not attributed; *p*: *p*-value of the χ^2 test. See Online Resource 1 for further information

Group	Sample size	French foxes				Australian foxes	
		Mandible form	Muscle mass	Muscle PCSA	BF	Mandible form	Muscle data and BF
'All'	N	64	60	58	56	433	14
	by sex	23 F, 37 M (4 NA)	23F, 36 M (1NA)	23F, 34 M (1NA)	22F, 33 M (1NA)	200 F, 232 M (1 NA)	6 F, 8 M
	χ^2 test	$p=0.07$ $\chi^2=3.3$	$p=0.09$ $\chi^2=2.9$	$p=0.15$ $\chi^2=2.1$	$p=0.14$ $\chi^2=2.2$	$p=0.12$ $\chi^2=2.4$	$p=0.6$ $\chi^2=0.29$
'Adults only'	N	52	50	49	47	175	14
	by sex	19 F, 30 M (3 NA)	19F, 29 M (1NA)	19F, 28 M (1NA)	18F, 28 M (1NA)	76F, 99 M	6 F, 8 M
	χ^2 test	$p=0.12$ $\chi^2=2.5$	$p=0.15$ $\chi^2=2.1$	$p=0.19$ $\chi^2=1.7$	$p=0.14$ $\chi^2=2.2$	$p=0.082$ $\chi^2=3.0$	$p=0.6$ $\chi^2=0.29$

semi-landmarks on curves, and 185 sliding semi-landmarks on the surface were placed on the mandibles of each specimen using the 'Landmark' software, version 3.0.0.6 (© IDAV 2002–2005, Wiley et al. 2005, Fig. 1, Online Resource 2).

All subsequent statistical analyses were run in R version 3.6.0 (2019–04-26) and R studio version 1.2.1335. Landmarks were transformed into homologous landmarks using an iterative sliding semi-landmark procedure implemented in the 'Morpho' package (version 2.7) implemented in R

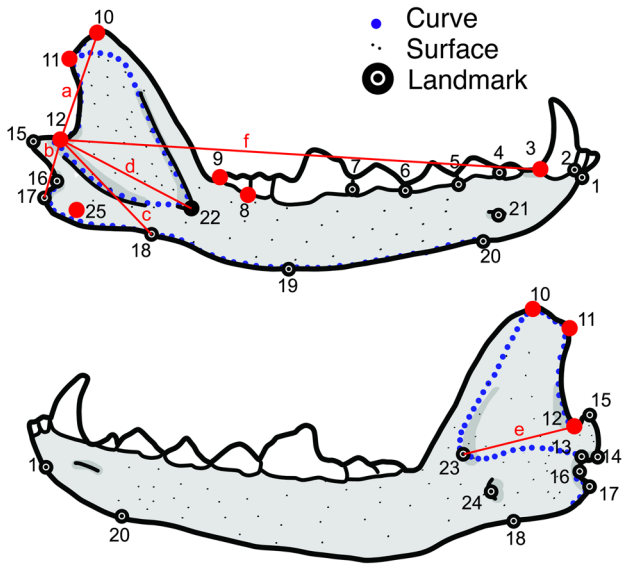

Fig. 1 Landmarks used in this study illustrated on the lateral and medial views of the mandible of a French red fox (*Vulpes Vulpes*). Definitions of the landmarks are provided in Online Resource 2. The landmarks and distances that are used for bite force prediction in Model 2 are illustrated in red. They correspond to the in-lever of the m. temporalis pars superficialis (**a**), the m. masseter pars superficialis (**b**), the m. masseter pars profunda (**c**), the m. temporalis pars suprazygomatica (**d**), the m. temporalis pars profunda (**e**) and the out-lever arm of the bite force vector at the canine (**f**)

(Bookstein 1991; Gunz et al. 2005; Schlager 2013). Generalized Procrustes analyses (GPAs; Rohlf and Slice 1990) and principal component analyses (PCAs) were performed using the function 'procSym' (Klingenberg et al. 2002; Gunz et al. 2005; Dryden and Mardia 2016). The deformation of the mandible of a French fox to the consensus of the GPA was used as a reference for all visualizations. In order to explore variation in the part of shape that does not depend on size, allometry-free shape coordinates were obtained from the functions 'CAC' (Mitteroecker et al. 2004) and 'plotTangentSpace'.

Study of Function

Dissection of Jaw Adductors In the present study, we dissected the jaw muscles in 14 adult red foxes from Pilbara in northern Australia (Table 1) following the method described in Brassard et al. (2020). We isolated 10 muscle bundles: m. digastricus, m. masseter pars superficialis and profunda, m. zygomaticomandibularis anterior and posterior, m. temporalis pars suprazygomatica, superficialis and profunda, and m. pterygoideus pars medialis and lateralis. For each bundle, we measured the mass (using a digital scale: Mettler Toledo AE100), the pennation angle, and the fibre length (directly on the muscle considering the mean of five measurements taken on different parts of the muscle). We used these data to calculate the reduced PCSA (Haxton 1944; Martin et al. 2020) as follows, using a density of 1.06 g cm^{-3} (Mendez and Keys 1960), a reliable estimate for use in the reduced physiological cross-sectional area (RPCSA) in the red fox (Penrose et al. 2020): $RPCSA = \frac{mass(g)*\cos(angle\ of\ pennation(rad))}{1{,}06(g.cm^{-3})*fiber\ length(cm)}$.

For 56 of the French foxes, muscle data were obtained from Brassard et al. (2021). To increase statistical power, we calculated mean fibre length, pennation angle, and the sum of

muscle masses and PCSAs for each muscular group (masseter, temporalis, and pterygoids).

Biomechanical Model to Estimate Bite Force in Australian Foxes For the French foxes, estimated bite forces, extracted from Brassard et al. (2021), were obtained by means of a biomechanical model using individual PCSAs of all muscles as well as the precise coordinates of attachment of all adductor bundles on the cranium and mandible obtained during dissection. For the 14 northern Australian red foxes, we used a simplified model (Fig. 2), as we could not use a microscribe during the dissection and because the skulls had some damage. Considering the low number of specimens, we grouped the main adductors (masseter, temporalis, and pterygoid) without distinguishing all the bundles. Muscle force magnitudes were obtained by multiplying the reduced PCSA by a conservative muscle stress estimate of 30 N cm^{-2} (Herzog 1994). We used photographs of dorsal and lateral views of the skulls, on which we drew the axes as follows: the X-axis running parallel to the sagittal axis of the cranium and passing by the right temporomandibular joint (the centre of the system); the Y-axis directed towards the top of the cranium and perpendicular to X; and the Z-axis running from the midline outwards, perpendicular to the other two axes (Fig. 2). In this frame of reference, we recorded the coordinates of the centroid of the origin and insertion areas of the main adductors without distinguishing the bundles based on observations from our dissections. We also recorded the point of application of the bite force at the canine tooth BPc for a gape opening of 20°. These coordinates were used to calculate the moment arms (the shortest distance between the centre of the system and the line of action of the force) for each muscle group and for the resulting force at the bite point (for an orientation of the force of -90°), and then finally the magnitude of the moment of each muscle/bite point, which corresponds to the numeric product of force magnitude and moment arm. Considering that at static force equilibrium, the sum of the moments of the external forces (force in the joint, force at the bite point, and force exerted by each muscle group) is zero, we could deduce the resulting bite force as follows: $BF_{two\ sides} = 2 \times \frac{\sum_{i=1}^{8} PCSA \times 30 \times ila}{ola}$, where *BF* represents the norm of the estimated bite force, *ila* is the length of the effective in-lever arm for each adductor muscle group and *ola* is the length of the effective out-lever arm at the bite point.

A preliminary correlation test ('cor.test') performed on the bite forces estimated using this simplified biomechanical model and those estimated using the original and more complex biomechanical model (data extracted from Brassard et al. 2021) for the 56 dissected French red foxes revealed that estimations are similar ($r = 0.89$). This simplified method thus provides a good approximation of the maximal bite force in the 14 Australian red foxes in comparison with the full model (Brassard et al. 2021) validated by in vivo bite force data.

Predictive Models of Bite Force Based on Mandible Form Using PLS Regressions Forbes-Harper et al. (2017) previously estimated bite forces at the canine using the dry skull

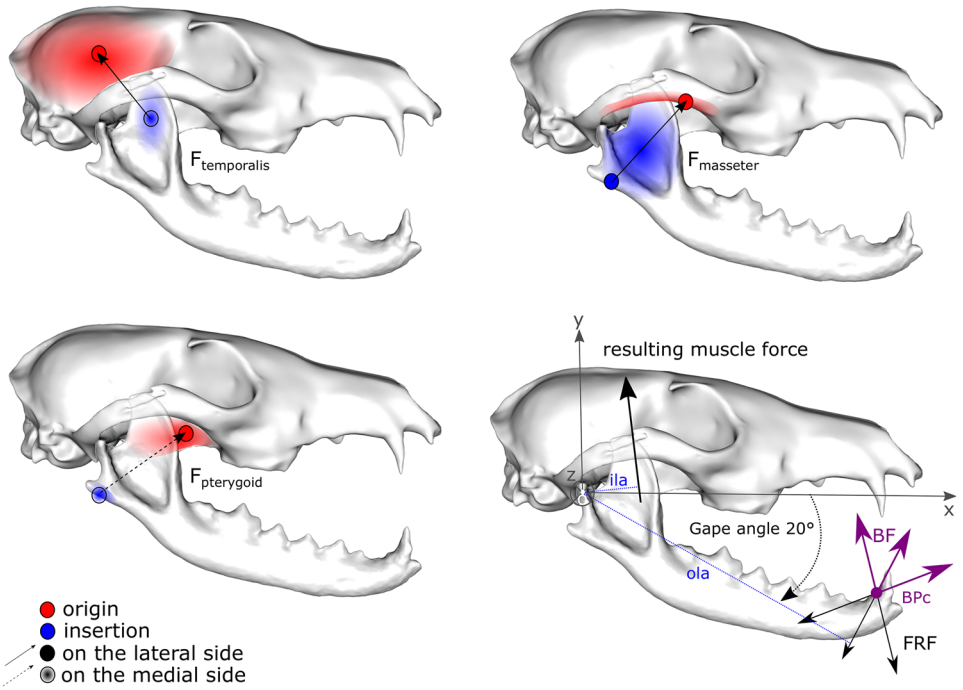

Fig. 2 Simplified biomechanical model used in this study to predict bite force using the individual architecture of the jaw muscle groups in 14 dissected Australian foxes (*Vulpes vulpes*). For each muscle complex, the attachment area on the skull is represented in red and that on the mandible is in blue. The landmarks corresponding to muscle attachments for the calculation of muscle moments are represented by open symbols when on the medial side. Abbreviations: BF: bite force; FRF: food reaction force; $F_{temporalis}$, $F_{masseter}$, and $F_{pterygoid}$: forces calculated from attachment coordinates and PCSA of the jaw adductors; ila: in-lever arm; ola: out-lever arm; BPc: bite point at the canine

method, which estimates muscle PCSA from dimensions taken on the skull and not architecture of the muscles per se. Here, we develop two predictive models to estimate the $\log_{10}$-transformed bite force at the canine for an intermediate gape angle of 20° (more realistic than an angle of 0°) and an orientation of the force perpendicular to the mandible. To establish the decision rules of the models, we used bite force data previously estimated using individual muscle architecture quantified from the dissection of 56 French red foxes and that had been validated with in vivo bite force measurements (Brassard et al. 2021). For these French foxes, estimated bite forces showed a strong correlation with mandibular shape and size (Brassard et al. 2021). For both models, we used the function 'plsR' from the package 'plsRglm' (Meyer et al. 2010), with leave-one-out cross validations. Model 1 used the Procrustes coordinates and the $\log_{10}$-transformed centroid size. A difficulty with this method is that the decision rules of the model need to be re-established each time new individuals are added to the sample (because all individuals, even the ones used for the prediction, need to be superimposed with the same GPA). Model 2 used only a few landmarks that correspond roughly to the point of insertion of the adductor muscles on the lower jaw, the centre of rotation of the mandible (condyle), and the point of application of the bite force (on the canine; Figs. 1 and 3). The lengths of the in-levers (Euclidean distances between the point of insertion of the muscle and centre of rotation) and out-levers (Euclidean distances between the canine and centre of rotation) were calculated based on the coordinates of these points (Fig. 3). The advantage of this second method is that it does not require a GPA. Previous studies revealed strong correlations and covariations between mandible shape and bite force in French foxes (Brassard et al. 2021). In order to quantify the exact amount of covariation used to build the decision rules of the two predictive models in our sample of French red foxes, we performed a two-block partial-least-square analyses using the function 'pls2B' (Rohlf and Corti 2000). The 2B-PLS calculated singular values and created a new PLS axis by looking for linear combinations in each block (block 1: mandibular form as predictor variables, block 2: vector of the $\log_{10}$-transformed estimated bite forces, as dependant variable) that maximise the covariance between blocks. A PLS coefficient ($r\text{-}_{PLS}$) was generated reflecting the degree of covariation, accompanied by a *p*-value providing significance of the covariation (calculated by comparing the singular value to those obtained from 1,000 permuted blocks).

The accuracy of each model was assessed by comparing the model outputs (predicted bite force) with the inputs (estimated bite force from dissections) for the 56 French (Brassard et al. 2021; this study) and 14 Australian foxes (this study) that we dissected. To do so, we performed correlation tests (with the function 'cor.test'), as well as two-sided t-tests to compare the means (function 't.test'). We also compared the two model outputs with estimates obtained previously from the dry-skull method, when available (n = 325 Australian red foxes; Forbes-Harper et al. 2017).

Estimation of Muscle Contribution to the Bite Force Calculation of the mechanical potential estimates the relative contribution of the different muscles to the bite force and thus brings complementary information to the predicted absolute bite force. The mechanical potential of each muscle corresponds to the ratio of the moment arm of the force exerted by the muscle over the lever arm of the resulting bite force at a given bite

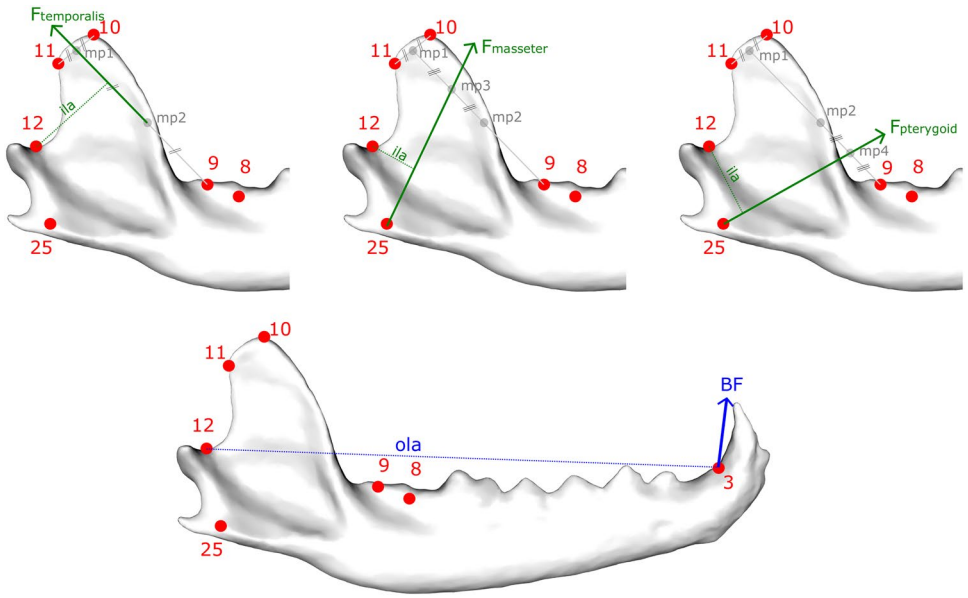

Fig. 3 Landmarks used to calculate the mechanical potential of the temporalis, masseter, and pterygoid muscles of red foxes (*Vulpes vulpes*) from Western Australia and France. Abbreviations: BF: bite force at the canine (landmark 3); Ftemporalis: force exerted by the temporalis muscle, Fmasseter: Force exerted by the masseter muscle, Fpterygoid: force exerted by the pterygoid muscle; ila: moment arm of the force exerted by the corresponding muscle (from landmark 12), ola: out-lever arm of the force exerted by the bite force at the canine tooth (between landmarks 3 and 12), mp: midpoints mentioned in the text

point (out-lever). Our method is based on that of Carraway et al. (1996), who calculated the mechanical potential of a muscle as the ratio of the in-lever (distance between the point of application of the muscle force and the centre of rotation of the system) and the out-lever arm (distance between the point of application of the bite force and the centre of rotation of the system). Here, we used a modified version of this method to take into account the muscle moment arms (that is to say the shortest or perpendicular distance between the centre of rotation of the system and the force vector) in the calculations (Cornette et al. 2012; Kouvari et al. 2021). We calculated the mechanical potential of the temporalis, of the masseter, and of the pterygoid muscles. For this purpose, we approximated the direction of the force exerted by each muscle from a few key landmarks whose raw coordinates (without Procrustes superimposition because we do not want to scale the bones, as size matters) were extracted prior to the GPA (Fig. 3). To represent the force exerted by the temporalis muscle we created a vector that takes its origin at the mid-point between landmark 9 and the middle between landmarks 10 and 11 (mp2), and the direction of which is given by the midpoint between landmarks10 and 11 (mp1). The perpendicular between this vector and the centre of rotation (landmark 12, ila) corresponds to the moment arm of the temporalis muscle. This assumes no variation in the origin of the muscle on the cranium. The moment arm thus depends on the inclination of the coronoid process relative to the axis of the mandible. The same way, the moment arm of the masseter muscle was calculated by creating a vector that takes its origin at the landmark 25 and whose direction is given by the midpoint between mp1 and mp2 (mp3). The moment arm of the pterygoid muscle was calculated by creating a vector that takes its origin at the landmark 25 and whose direction is given by the midpoint between landmark 9 and mp2 (mp4). The moment arms of the masseter and pterygoid muscles thus depend on the shape of both the angular and coronoid processes. We considered that the out-lever arm was the distance between the centre of rotation of the system (landmark 12) and the caudal border of the alveolus of the canine tooth (landmark 3, ola). It is therefore assumed that the bite force is oriented perpendicular to this line. The mechanical potential of each muscle at the canine was calculated as the ratio of the in-lever moment arm (ila) to the out-lever moment arm (ola), and the contribution of each muscle to the bite force was estimated as the ratio of the mechanical potential of each muscle to the sum of the mechanical potential of the three muscles (in percent). For analyses we used the $\log_{10}$-transformed value of muscle contributions.

Statistical Analyses

The centroid size, muscle mass, muscle PCSAs, and estimated or predicted bite forces were $\log_{10}$-transformed before analyses to normalize data. Residual muscle mass, muscle PCSA, or estimated or predicted bite forces were obtained from the regression of the $\log_{10}$-transformed muscle mass, muscle PCSA or bite forces (respectively) on the $\log_{10}$-transformed centroid size of the mandible, using the function 'lm'.

To test whether Australian and French foxes differ in mean mandible size, we performed a Welch two sample t-test in case variances were unequal between groups. The variability in size between groups was compared with the function 'var.test'. To test whether Australian and French foxes differ in mean mandible shape, we performed a Procrustes analysis of variance (Procrustes ANOVA) using the function 'procD.lm' from the geomorph package (Hand and Taylor 1987; Krzanowski 1988). We further compared the mean shapes with a canonical variate analysis using the function 'CVA' (Campbell and Atchley 1981; Klingenberg and Monteiro 2005). A classification rate was obtained after a leave-one-out procedure. Shapes at the minimum and maximum of the CV axis were obtained, as well as the vectors of deformation between them (using the function 'deformGrid3d'). To compare the variability in shape, disparity tests were conducted using the function 'morphol.disparity' from the geomorph package (Foote 1993; Zelditch et al. 2012), so as to take into account the difference in sample size between groups. Morphological disparity was estimated as the Procrustes variance in each group, using residuals of a linear model fit (the sum of the diagonal elements of the group covariance matrix is divided by the number of observations in the group). Pairwise comparisons between groups and associated *p*-values were obtained after 1,000 permutations that randomized the vectors of residuals among groups. We performed analyses on the total sample (thus including the youngest foxes) and on the group with adult foxes only, the latter minimizing variation due to growth allometry. We performed analyses on the raw shape as well as on the allometry-free shape.

To test whether genetic drift is responsible for the differences in mandible shape between French and Australian foxes, we used the method proposed by Le Maître and Mitteroecker (2019) implemented in the vcvComp package (see details in the Online Resource 3). To do so, we first compared the covariance matrices of the two populations. The scores of the first five principal components performed on the GPA coordinates of all adult foxes were used to compute the covariance matrix for each population. We then performed a ML test of proportionality between these two covariance matrices and computed the ratio of generalized variances of European with respect to Australian populations using function relGV.multi. Upon rejection of the hypothesis of proportionality, a relative principal component analysis (relative PCA) was performed to compare the two covariance matrices based on their relative eigenvalues and eigenvectors. We tested whether the first and last relative eigenvalues differed, supporting a separate interpretation of the

corresponding relative eigenvectors. Finally, we explored the shape patterns corresponding to the first and last relative eigenvectors to explore what discriminant traits are under divergent or stabilizing selection. In a second step, we performed similar analyses to compare the between- (B) and within- (W) population covariance matrices.

To explore the differences in the muscle architecture between Australian and French foxes, we performed principal component analyses (function 'PCA' from the package 'FactoMineR'), as well as two-sided t-tests (function 't.test'), on the ($\log_{10}$-transformed) proportions of the mass or PCSA of each muscle bundle to the total mass or PCSA of the adductor muscles.

We compared the variation in bite force or residual bite force and the relative contribution of each muscle group to bite force in adults between the French and the Australian populations with t-tests (function 't.test').

Results

Validation of the Two Predictive Models of Bite Force and Comparison With the Dry Skull Method

As previously demonstrated (Brassard et al. 2021), strong covariations between mandible form and bite force exist, whether we take into account the complete 3D shape (Model 1: $r\text{-}_{PLS} = 0.81$, $p < 0.001$) or the linear measurements (Model 2: $r\text{-}_{PLS} = 0.72$, $p < 0.001$; Fig. 4). Additionally, we observed that the variability in the part of the mandible that covaries with bite force in French foxes encompassed the variability of the sample of 14 Australian foxes (for which we want to predict bite forces; Fig. 4). The two predictive models based on PLS regressions were thus applicable to the data for the Australian foxes.

Predicted bite force (predBF) and estimated bite force (BF) showed good correspondence for both models used to establish the decision rules for the 56 French red foxes (Table 2). There was a stronger correlation for data derived with Model 1, which used more accurate shape information (Table 2, Fig. 4). However, there was no difference in the bite force estimations derived from dissections (Model 1) and predictions based on PLS regressions (Model 2, t-test: $p > 0.7$; Fig. 5).

For the 14 Australian dissected red foxes, the correlation between estimated bite force (BF) and predicted bite force (predBF) was only significant for Model 1. The low correlation coefficient is likely because of the small sample size and the slightly different method used to record the coordinates of muscle area attachment on the cranium and mandible (compared with the more complete biomechanical model used to estimate bite force in the French foxes used to build the decision rules; Brassard et al. 2021). The results are poor for Model 2, suggesting that the few Euclidean distances between landmarks were insufficient to capture relevant variation required to accurately estimate bite force. A comparison of the mean bite force between estimations from dissections and predictions based on PLS regressions for the 14 dissected Australian foxes suggest that Model 2 tended to overestimate the bite force ($p = 0.007$) whereas there was no significant difference for Model 1 ($p = 0.1$; Fig. 5).

Bite forces predicted from the two PLS regression models are correlated with estimates obtained previously using the dry skull method (Table 2). Interestingly, the correlation is better with Model 2, which uses simple Euclidean distances, perhaps because it is more similar to the dry skull method and also tends to overestimate bite force (by around 20 N; see Fig. 5). The comparison of mean predicted bite forces (t-test) reveals that the dry-skull method significantly overestimates bite force ($p < 0.001$; Fig. 5).

Comparison of Mandible Form Between Native and Invasive Foxes

The comparison of adult foxes reveals that French red foxes tend to be slightly smaller than adult Australian foxes on average (Table 3, Fig. 6), but there is no difference in the size variance in foxes from the same region. Disparity tests performed on the shapes or allometry-free shapes of adults suggest that native and invasive foxes show a similar degree of variation, which is also observable on the two first axes of the PCA (Fig. 6). The difference becomes significant when juvenile or young foxes of under 1 year of age are included (the French foxes show greater variability than Australian foxes, yet they are less numerous; Table 3).

The comparison of mean shapes reveals strong differences between French and Australian foxes, both when examining only adults and all individuals, irrespective of whether analyses are performed on shape or allometry-free shape. This suggests that differences depend on more than just gross size differences between the two groups. The CVA easily distinguished the two populations (the cross-validation lead to excellent success rates; Table 3). If only adults are considered, French foxes have longer, slenderer, and thinner mandibles, with a more triangular coronoid process, a deeper masseteric fossa, and a bigger angular process and condyle (Fig. 7) compared to Australian foxes. Most of these differences are not due to allometry, as the same observation can be made for allometry-free shapes (except for the differences in the length of the mandible; Fig. 7). The morphological differences are located in functionally important areas (Brassard et al. 2021) and are likely accompanied by functional differences.

The ML test further indicates that the covariance matrices of Australian and French foxes are not proportional ($p < 0.001$; see Online Resource 3), suggesting stabilizing or

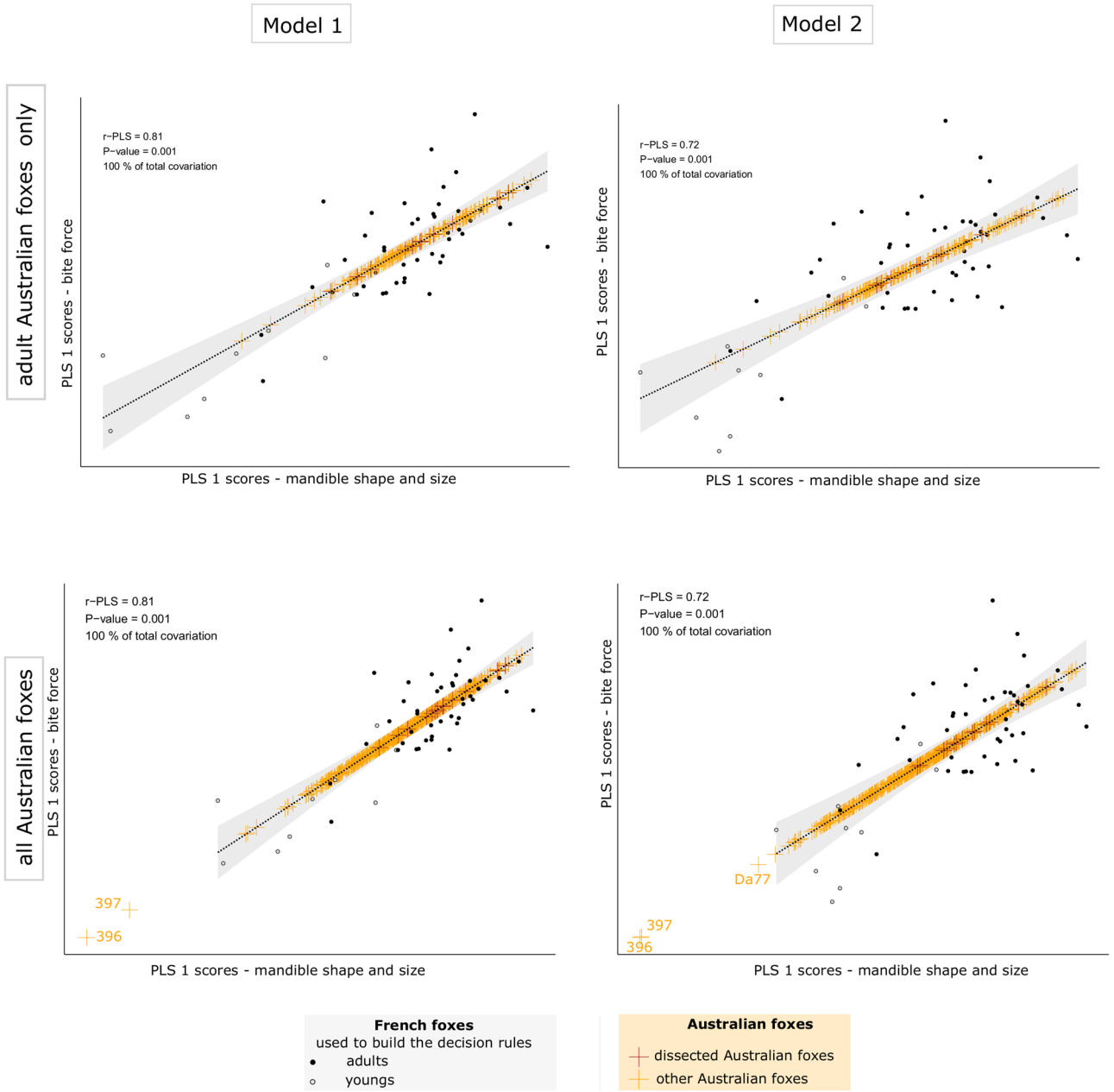

Fig. 4 Covariation between mandible form and estimated bite force in French red foxes (*Vulpes vulpes*). PLS equation used to build the two predictive models (in dots and black) with projection of the Australian foxes (dark red and orange crosses). Model 1: predictions are based on mandible shape and centroid size; Model 2: predictions are based on Euclidean distances between landmarks. The coefficient of covariation (r-PLS) with the corresponding *p*-values are reported. The regression lines corresponding to the predictive models are shown. The grey bands around the line represent the standard error of the regression line. The three labelled Australian foxes which stand outside the variability of the predictive model correspond to foxes with body masses and mandible forms compatible with the most juvenile foxes (Online Resource 1)

divergent selection (Le Maître and Mitteroecker 2019). The generalized variance of French foxes was only 2% higher than that of Australian foxes, but the relative PCA showed that the various shape features deviate strongly in their variational properties across populations (Online Resource 3: Fig. S1). The first relative PC was roughly 1.9 times more variable in French foxes than in Australian foxes (first relative eigenvalue was 1.9), whereas the variance of the last relative PC in French foxes was only half that of Australian foxes (last relative eigenvalue was 0.58; Online Resource 3: Fig. S1a). The shape features captured by relative PC 1 (with maximal excess of variance in the French populations

Table 2 Correspondence between red fox (*Vulpes vulpes*) bite forces predicted from the two predictive models based on PLS regressions (predBF) and bite force estimated from dissections (BF) or bite forces predicted from the dry skull method ($predBF_{dsm}$ from Forbes-Harper et al. 2017). Model 1: predictions are based on mandible shape and centroid size; Model 2: predictions are based on Euclidean distances between landmarks. *p*: *p*-value of the correlation test between predBF and BF or $predBF_{dsm}$; *r*: coefficient of correlation; Adjusted *p*: adjusted *p*-value from the Tukey post-hoc test performed to test for differences between the estimated BF and predBF

		predBF – BF		**predBF – $predBF_{dsm}$**
Sample		French red foxes	Australian red foxes	
Sample size		56 dissected	14 dissected	All 325 foxes
Results for Model 1	*p*	< 0.001	0.046	< 0.001
	r	0.84	0.54	0.70
	adjusted p	0.9	/	< 0.001 $predBF_{dsm}$ > predBF
Results for Model 2	*p*	< 0.001	0.6	< 0.001
	r	0.76	0.13	0.80
	adjusted p	0.9	0.007 mean predBF > mean BF	< 0.001 $predBF_{dsm}$ > predBF

relative to Australian populations) were the shape of the coronoid and angular processes and the height and thickness of the anterior part of the mandibular body (Online Resource 3: Fig. S1b). In other words, these are the shape features maximally canalized in the invasive population. On the contrary, mandible length and coronoid process height were the shape features with maximal excess of variance in the Australian populations relative to the French populations (which means they were less canalized in the invasive population; Online Resource 3: Fig. S1c). With respect to the analyses performed on the within and between covariation matrices, the ML test suggests once again strong deviation

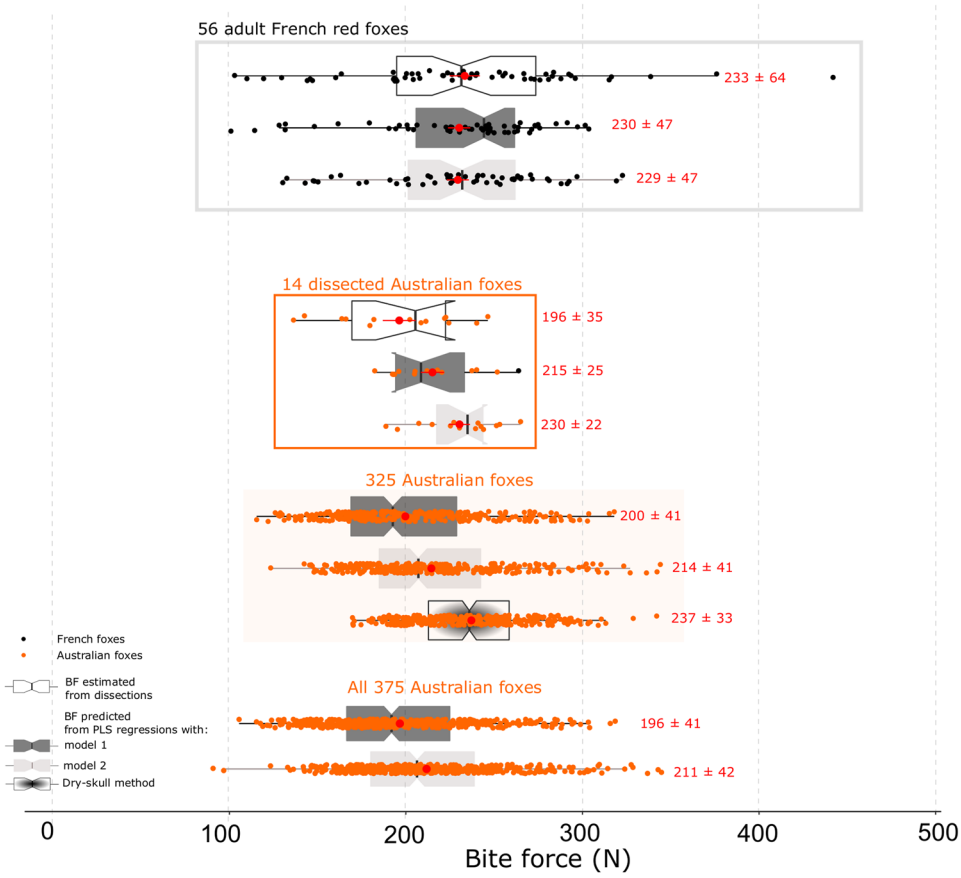

Fig. 5 Variation in the bite force estimated from dissections and bite forces predicted from the two predictive models based on PLS regressions (predBF), or bite forces predicted from the dry skull method (from Forbes-Harper et al. 2017) for the dissected French red foxes, the dissected Australian foxes, and all the Australian foxes with predictions from the dry skull method. Different colours are used for the different groups of foxes and for the different methods. The mean and standard deviation are indicated in red. Model 1: predictions are based on mandible shape and centroid size; Model 2: predictions are based on Euclidean distances between landmarks

Table 3 Results of the analyses to test for differences in mandible centroid size and shape between French and Australian red foxes (*Vulpes vulpes*). Abbreviations: Fr: France; Au: Australia; Var: Variance; *p*: *p*-value

	Sample size		CENTROID SIZE		SHAPE						
					Disparity test			Mean shape			
					Procrustes variance			Procrustes Analyses			CVA
	Fr	Au	Var	Mean	Fr	Au	*p*	R^2	*F*	*p*	
Shape											
All	64	433	0.3	0.8	0.0039	0.0034	0.027	0.023	11.4	< 0.001	97%
Adults only	52	175	0.2	0.024 Fr < Au	0.0035	0.0033	0.3	0.038	8.9	< 0.001	99%
Allometry-free shape											
All	64	433			0.0034	0.0030	0.012	0.025	12.9	< 0.001	/
Adults only	52	175			0.0028	0.0026	0.2	0.028	6.4	< 0.001	91%

from proportionality ($p < 0.05$). The first relative PC (which eigenvalue is 0.73) corresponds to the slenderness and curvature of the mandibular body and the shape of the coronoid and angular processes. The deformations described in this paragraph are similar to those observed in the CVA (Fig. 7 and Online Resource 3: Fig. S1).

Comparison of Muscle Architecture (Mass, PCSA) Between Native and Invasive Foxes

The analyses of muscle data obtained from the dissection of the 14 adult foxes from Australia and the comparison with data available in 50 adult foxes from France revealed that Australian foxes have a relatively less voluminous temporalis muscle that has a lower PCSA but more voluminous masseter and pterygoid muscles with a greater PCSA (Fig. 8).

Comparison of Predicted Bite Force Between Native and Invasive Foxes

Adult Australian red foxes have lower bite forces compared to the French foxes, even relative to mandible centroid size (Table 4). However, there is a strong overlap between the two groups, and the variability in the data is important (Fig. 9).

Comparison of the Relative Contribution of Each Muscle Group to Bite Force

When the contribution of each muscle to the bite force is estimated for the adult red foxes, the temporal muscle contributes more to the bite force in Australian foxes than in French foxes ($p = 0.027$, Fig. 9). In French foxes, the masseter contributes more to the overall bite force compared to Australian foxes ($p = 0.007$, Fig. 9).

Discussion

Predictors of Bite Force

In this study, we developed two predictive models of bite force based on the relationship between mandible form and bite force using data obtained from the dissection of French red foxes. When applied to the Australian red foxes, the bite force predictions obtained using both models showed a strong correlation with bite force estimates obtained from the dry-skull method. The dry-skull method has been shown to be less accurate as it does not take into account muscle architecture nor the 3D geometry of the skull (Davis et al. 2010) and tends to overestimate bite force by around 20 N (Fig. 4). We obtained a closer correspondence for the model based on Euclidean distances due to the similarity with the dry-skull method, yet both overestimated bite force when compared to estimates based on dissections. The model which used all surface landmarks is more accurate, as it considers the 3D shape of the mandible. This was confirmed by the apparent good correspondence between the estimated bite force (using a 3D lever model based on dissection data) and PLS predictions using the complete mandible form in the dissected foxes. However, the small sample size of the dissected Australian foxes could bias this result since they did not cover the full range of morphological variation spanned by Australian foxes (in terms of mandible size, shape, and muscle architecture; Fig. 6). These methods do, however, offer interesting perspectives for applications in other contexts, including comparisons with the fossil record. Unfortunately, in this study, we could not use all the different methods to estimate bite force (dry-skull, PLS predictions, dissection) for the entire sample. A future study comparing model outputs is needed to investigate the accuracy and the relevance of each method further.

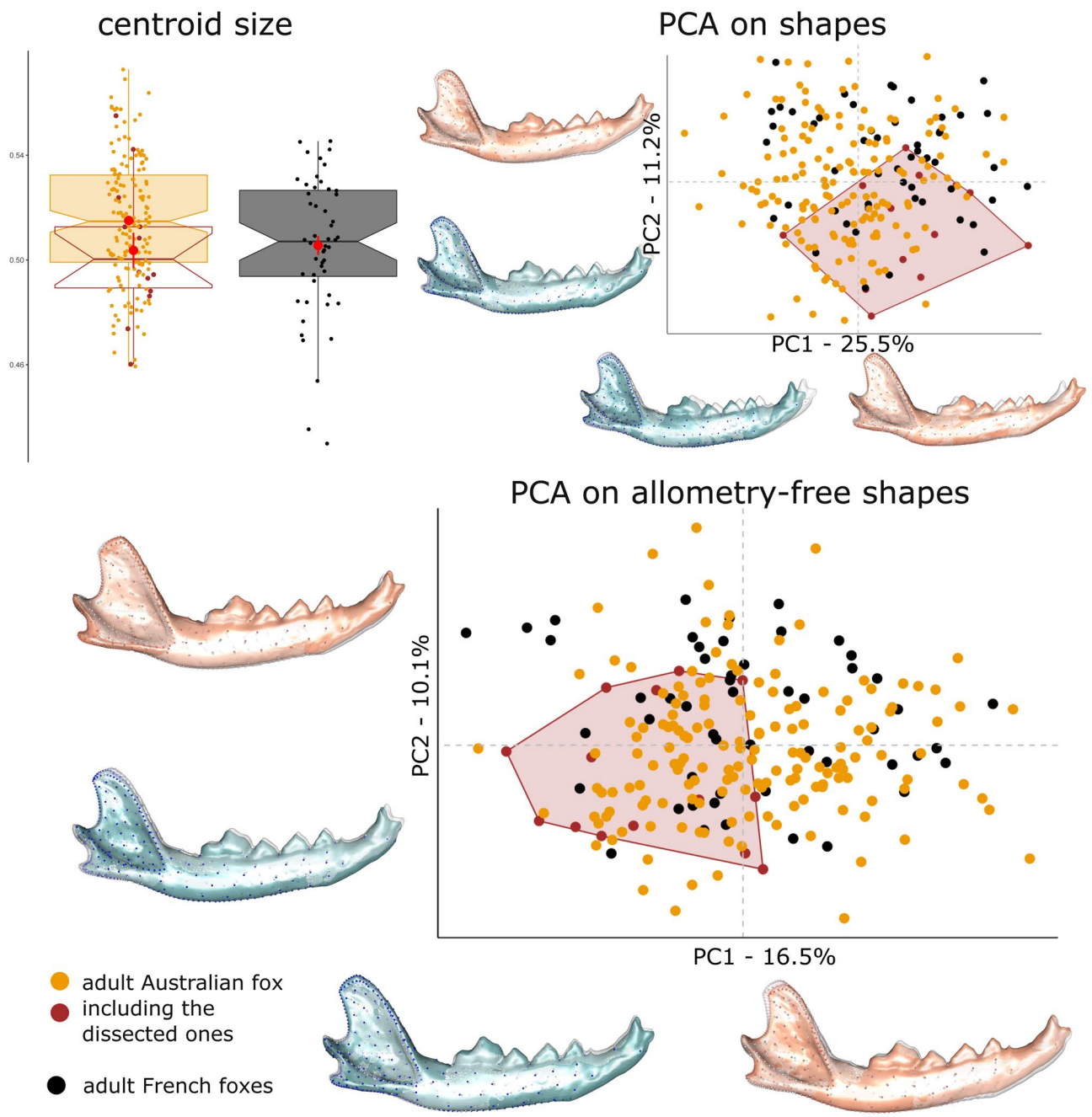

Fig. 6 Visualisation of the variability in mandible size, shape and allometry-free shape in adult red foxes (*Vulpes vulpes*) from Australia (n = 175) and France (n = 52), with lateral views of the shapes at the minimum (blue) and maximum (orange) of the PC axes, superimposed to the shape of the consensus (white) with the vectors of deformations

Differences Between Australian and French Foxes

In this study, using 3D geometric morphometrics and jaw muscle dissection, we demonstrated significant differences in mandibular shape and size, muscle architecture, and jaw function between Australian and French red foxes. First, our results demonstrated a reduced disparity in invasive Australian foxes when the youngest foxes are taken into account in the analyses, and strong differences in mean mandible shape (and size, at least for adults). A strong differentiation between native European and invasive Australian populations thus seems to have occurred. These results may be due to founder effects, as relatively few individuals were introduced (Allendorf and Lundquist 2003; Saunders et al. 2010). Consequently, it is possible that the morphology of the individuals introduced (founders) was different, on

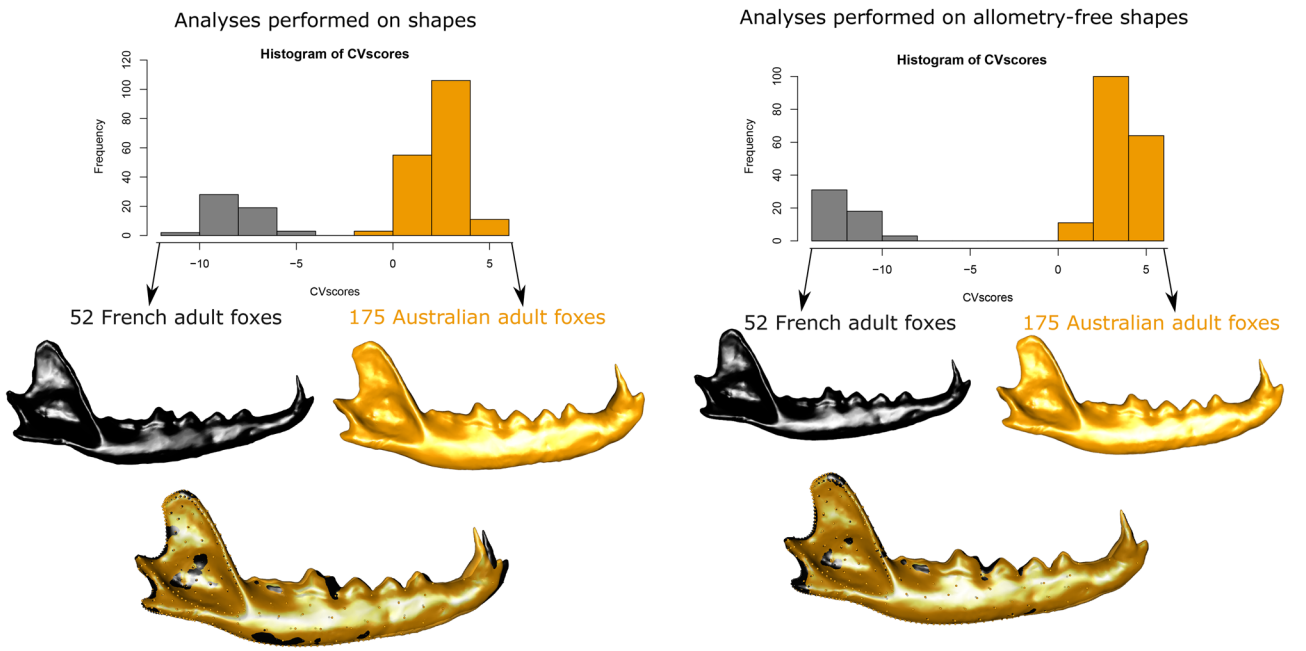

Fig. 7 Visualisation of the differences in shape or allometry-free shape of the mandible between native and invasive red foxes (*Vulpes vulpes*): histogram of CV-scores with lateral views of the theoretical shapes corresponding to the minimum and maximum of the CV-scores, either represented separately (differences from the consensus were magnified by three) or superimposed upon each other

average, from that of the source population, resulting in persistent differences over time (corresponding to genetic drift).

However, the results of the covariance comparisons are in favor of a strong divergent selection between populations. Under neutral evolution (pure genetic drift), the variance ratio of the between- (B) and the within- (W) population covariance matrices can be estimated based on genetic data (depending on the number of generations since divergence as well as the effective population size; Lande 1979; Le Maître and Mitteroecker 2019) using the F_{ST} statistic (Holsinger and Weir 2009; Le Maître and Mitteroecker 2019) estimated as B/W = FST/(1-FST) (Martin et al. 2008). Atterby et al. (2014) report F_{ST} values for European foxes (from United Kingdom and northern France) ranging from 0.004 to 0.181, which translates to ratios of between- and within-population variance of 0.004 – 0.22. In our analyses, the first relative eigenvalue (0.73) clearly exceeded this threshold, thus suggesting strong divergent selection. However, the results are to be taken with caution given the small number of populations included in our study. The shape of the coronoid and angular processes and the height and thickness of the anterior part of the mandibular body (Online Resource 3: Fig. S1b) were the shape features maximally canalized in the invasive population, contrary to mandible length and the height of the coronoid process.

These traits, contributing to the differences in mean mandible shape and bite force (and thus to feeding and defensive abilities) between the two populations, could thus be the result of stabilizing selection on a specific morphology that provides some functional advantage within the invasive population. Australian red foxes may have had strong selection pressures placed on them as they spread across the continent, especially crossing deserts. Foxes with a more efficient metabolism may have been favored, allowing better water conservation; for example, this could manifest as an optimal body surface area to volume ratio. However, our results are not compatible with Bergmann's rule, as centroid size of the mandible (which is positively correlated with body mass; $r = 0.62$, $p < 0.001$, N = 161 Australian foxes, using data from Forbes-Harper et al. 2017) was found to be slightly greater in Australian foxes compared to French foxes. This may also be related to differences in diet between European and invasive Australian populations. Indeed, the diet of invasive foxes frequently includes a significant amount of large carrion (Forbes-Harper et al. 2017), while that of European foxes is mostly made up of small mammals (Cavallini and Volpi 1996), and that of French foxes is not known to include large carrion (Castañeda et al. 2020). This is supported by the concentration of the anatomical differences in functionally important areas, as well as by the significant differences in mean predicted bite forces and the contribution of the muscles to the bite force. Invasive Australian foxes tend to have bigger and more 'dog-like' mandibles, with a more robust mandibular body and a more rectangular coronoid process (even once allometries are removed). They further produce slightly lower bite forces, on average, even

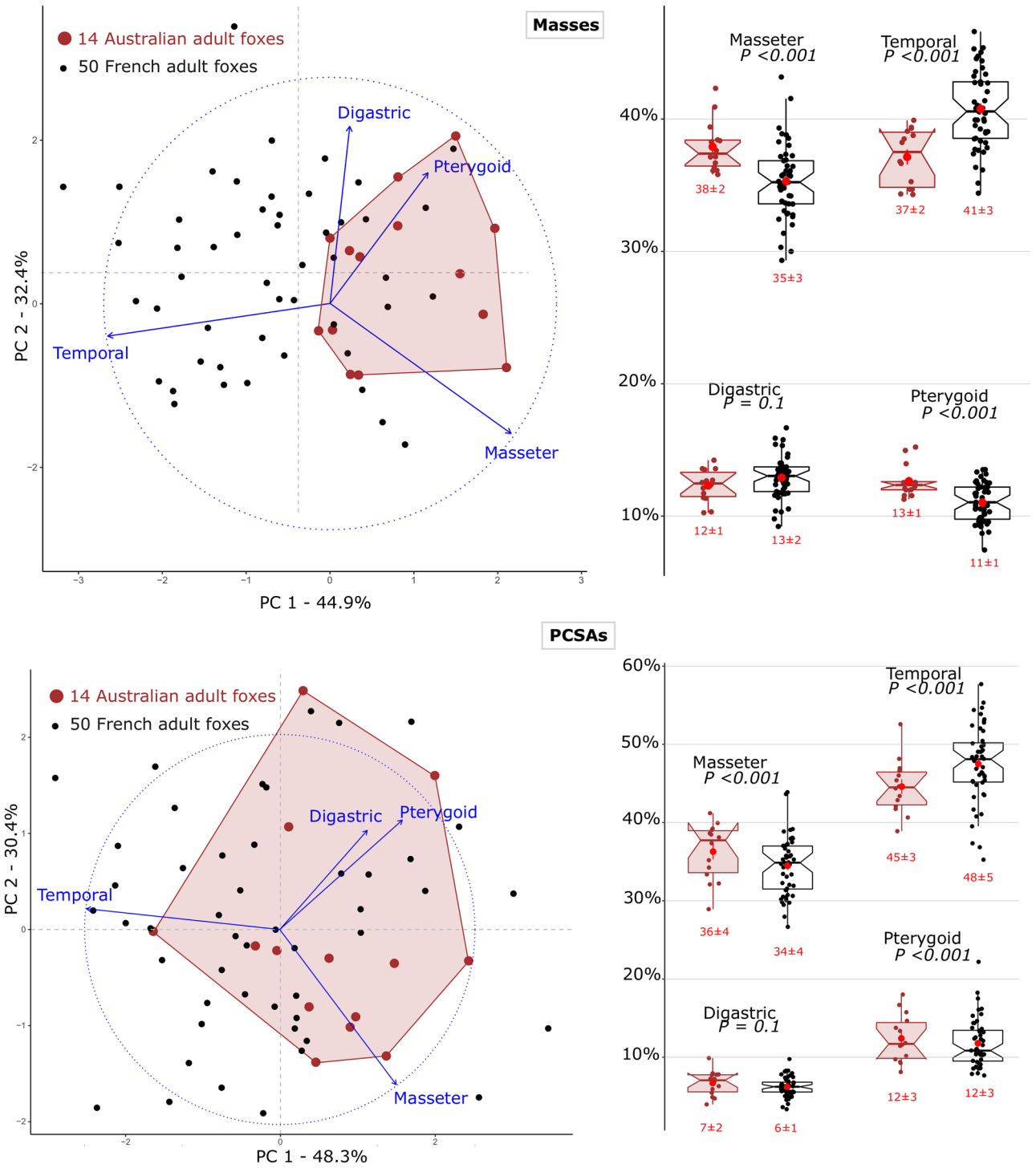

Fig. 8 Comparison of muscle architecture based on mass (above) or PCSA (below) in adult red foxes (*Vulpes vulpes*) from France and Australia. Left side: visualisation on the first two axes of the PCA with the variables factor map projected onto it. Right side: distribution of values for each muscle group with the mean and standard deviation (in red) and the result of the t-test performed to compare Australian and French groups (P: *p*-value)

when corrected for differences in size. This is compatible with the large proportion of carrion, which dries quickly in arid and hot climates, in the diet of the population included in our study (Forbes-Harper et al. 2017). Most interestingly, the mechanical advantage of the temporalis muscle and its contribution to bite force is greater in the Australian foxes

Table 4 Results of the analyses to test for differences in the absolute or residual predicted bite force between French and Australian red foxes (*Vulpes vulpes*). Fr: France; Au: Australia; Var: Variance; *p*: *p*-value

Sample	Sample size		Absolute estimated bite force				Residual bite force
	Fr	Au	Mean Fr	Mean Au	Var – *p*	Mean – *p*	*p*
All	64	433	229 ± 48 N	196 ± 41 N	0.06	< 0.001	< 0.001
Adults only	52	175	245 ± 29 N	231 ± 33 N	0.1	0.0025	< 0.001

than in French foxes. This is once again compatible with the large proportion of carrion in the diet of the Australian foxes: eating larger food items is associated with having jaws more adapted to biting at high gapes (Brassard et al. 2021). The relatively lesser importance of temporalis muscle PCSA and volume in the dissected foxes further suggests that the anatomical differences in the 3D shape of the skull are of great importance to explain the greater mechanical advantage of this muscle and thus its higher contribution in bite force. However, as we dissected few Australian foxes (they represent only a small part of the variability in the Australian group; see Fig. 7), the smaller contribution of the temporalis muscle to the total mass or PCSA of the jaw muscles needs to be confirmed with a larger sample. In contrast, French foxes have a more slender mandible with a deeper masseteric fossa, which is associated with a greater contribution of the masseter to the bite force. These foxes may thus be well suited to capture small mammals and insects and may not need to bite at large gape. As the data available suggest that French foxes hunt more live prey than Australian foxes, it also makes sense that they may be more adapted to produce greater bite forces relative to their size to capture and kill prey.

It is also possible that the release from the selective pressure of other predator species or the presence of naïve prey (marsupials, some other small and medium-sized native

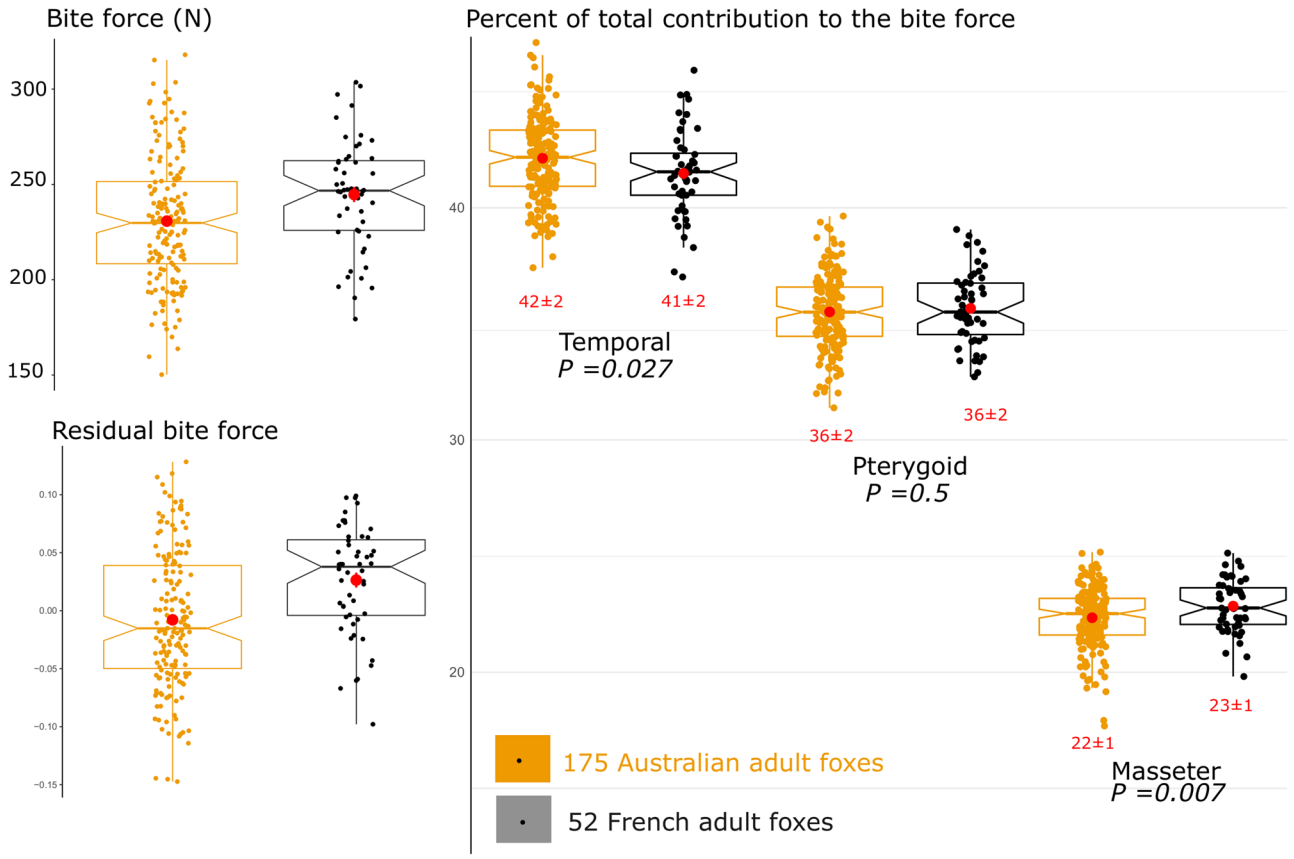

Fig. 9 Comparison of bite force, residual bite force, and estimated percentage of the total contribution of the different muscles to the bite force in adult red foxes (*Vulpes vulpes*) from France and Australia, with mean values and standard deviation (in red) and the result of the t-test performed to compare Australian and French groups (P: *p*-value)

mammals or birds) may have not favored foxes with greater bite forces. In particular, as marsupials had no evolutionary history with a fox-like predator prior to their introduction, they may not have developed adaptive antipredator behaviours (Dickman 1996; Sih et al. 2010). Low bite force may thus be sufficient to catch these naïve prey. Moreover, foxes have more natural competitors in Europe (golden eagle, badgers, domestic dogs, Eurasian lynx, and wolves) than in Australia (dingoes and feral cats; Robley et al. 2004; Sillero-Zubiri et al. 2004). Foxes are more abundant where dingoes and feral cats are less numerous (Newsome and Coman 1989; Catling and Burt 1995), reflecting competitive interactions for food and direct predation (Dickman 1996). Where present, dingoes seem to limit the access of foxes to resources (Fleming et al. 2001). Foxes, in turn, may competitively exclude feral cats from other food resources (Robley et al. 2004). Numerous studies attest to the important overlap in the diet of these three mesopredators (e.g. Catling 1988; Doherty et al. 2015, 2019; Fleming et al. 2021). All feed on rabbits, birds, reptiles, rodents, invertebrates, and plant material, but foxes generally have a broader diet. They prefer smaller items compared to the dingo (Cupples et al. 2011), which prefer large native mammals, principally macropodids (Doherty et al. 2019). Yet, foxes consume much more carrion than feral cats, who also prefer smaller prey (Doherty et al. 2015; Fleming et al. 2020, 2021). The lower number of competitors in Australia compared to France may have caused a release in selection pressures surrounding bite force, with low bite forces being sufficient to catch naïve prey and compete with relatively few other predators.

Comparison of other invasive and native populations of red foxes are rare. The few that do exist focus on North America, where invasive red foxes (voluntarily introduced from Europe for sport hunting during the middle 1700s and later) coexist with native red foxes, even though the former tend to replace the latter (Kamler and Ballard 2002). In the United States, native and invasive foxes differ deeply in color, ecology (native red fox habitats prefer locations at high elevations whereas invasive red foxes have a broader range of habitats and prefer low elevations), and morphology (invasive red foxes are larger, on average; Kamler and Ballard 2002), but no study has explored the differences further, especially with regards to bite force or cranial and mandibular shape.

Although divergence in mandible morphology between French and Australian foxes could be related to founder effects and genetic drift, the different geographical origin of the Australian foxes (other than France) could be part of the explanation. Unfortunately, it is very difficult to obtain accurate records on the subject (Abbott 2011). Our results are also consistent with divergent selection acting upon different parts of the mandible, allowing the consumption of different food items. Future studies investigating more specifically the relations between the proportions of different food items in the diet, bite force (see Forbes-Harper et al. 2017), and mandible shape in the invasive population or exploring variation in fossils may be particularly useful for better understanding whether the observed differences are indeed adaptive. However, differences due to different selective pressures related to climate (including temperature, precipitation, elevation, and topography), competition with other carnivores (Fischer and Still 2007; Spalding et al. 2007; Funk et al. 2016), sexual dimorphism, or the effects of phenotypic plasticity (Gortázar et al. 2000; Parsons et al. 2020) may potentially also drive variation in mandibular shape, reflecting differences in ecology. This remains to be investigated.

Supplementary Information The online version contains supplementary material available at https://doi.org/10.1007/s10914-021-09593-2.

Acknowledgements We thank the Veterinary school ONIRIS-Nantes (France), ANSES (Nancy, France), and Veterinary school of Life Science (Murdoch University, Australia) for providing access to fox mandibles. We also thank Arnaud Delapré for his help with photogrammetry. We are very grateful to the two anonymous reviewers for their comprehensive and constructive comments on an earlier version of this manuscript.

Author Contributions Colline Brassard and Anthony Herrel planned the study, collected data on the prepared dry bones and wrote the first draft of the paper. Colline Brassard analysed the data with assistance from Raphaël Cornette. All authors contributed to revisions. Colline Brassard, Marilaine Merlin, Jesse L. Forbes-Harper, Heather M. Crawford, John-Michael Stuart, Hélène Garès, Arnaud Larralle, Raymond Triquet collected the original material. Natalie M. Warburton, Michael C. Calver, Peter Adams, Patricia A. Fleming, Elodie Monchâtre-Leroy, Jacques Barrat, Sandrine Lesellier, Claude Guintard and Anthony Herrel oversaw field data collection. All authors approved the final version of the manuscript.

Funding This research was funded by a doctoral fellowship provided by the Ministère de l'Enseignement supérieur, de la Recherche et de l'Innovation and redactional time was funded by a post-doctoral fellowship from the Fyssen Foundation.

Data Accessibility Supplementary information about the sample are available in Online Resource 1. All code and 3D models used in this manuscript are available from the authors on request.

Declarations

Competing Interests The authors declare no conflicts of interest.

References

Abbott I (2011) The importation, release, establishment, spread, and early impact on prey animals of the red fox *Vulpes vulpes* in Victoria and adjoining parts of south-eastern Australia. Aust Zool 35:463–533. https://doi.org/10.7882/AZ.2011.003

Allendorf FW, Lundquist LL (2003) Introduction: population biology, evolution, and control of invasive species. Conserv Biol 17:24–30. https://doi.org/10.1046/j.1523-1739.2003.02365.x

Atterby H, Allnutt TR, Macnicoll AD, et al (2014) Population genetic structure of the red fox (*Vulpes vulpes*) in the UK. Mammal Res 60:9-19 . https://doi.org/10.1007/s13364-014-0209-6

Bookstein FL (1991) Morphometric Tools for Landmark Data. Geometry and Biology, Cambridge University Press, Cambridge

Brassard C, Merlin M, Monchâtre-Leroy E, et al (2021) Masticatory system integration in a commensal canid: interrelationships between bones, muscles and bite force in the red fox. J Exp Biol 224:jeb224394. https://doi.org/10.1242/jeb.224394

Brassard C, Merlin M, Monchâtre-Leroy E, et al (2020) How does masticatory muscle architecture covary with mandibular shape in domestic dogs? Evol Biol 47:133–151. https://doi.org/10.1007/s11692-020-09499-6

Campbell NA, Atchley WR (1981) The geometry of canonical variate analysis. Syst Zool 30:268–280. https://doi.org/10.2307/2413249

Carraway LN, Verts BJ, Jones ML, Whitaker JO Jr (1996) A search for age-related changes in bite force and diet in shrews. Am Midl Nat 231–240. https://doi.org/10.2307/2426705

Castañeda I, Zarzoso-Lacoste D, Bonnaud E (2020) Feeding behaviour of red fox and domestic cat populations in suburban areas in the south of Paris. Urban Ecosyst 23:731–743. https://doi.org/10.1007/s11252-020-00948-w

Catling PC (1988) Similarities and contrasts in the diets of foxes, *Vulpes vulpes*, and cats, *Felis catus*, relative to fluctuating prey populations and drought. Wildl Res 15:307–317. https://doi.org/10.1071/wr9880307

Catling PC, Burt RJ (1995) Why are red foxes absent from some eucalypt forests in eastern New South Wales? Wildl Res 22:535–545. https://doi.org/10.1071/WR9950535

Cavallini P, Volpi T (1995) Biases in the analysis of the diet of the red fox *Vulpes vulpes*. Wildl Biol 1:243–248. https://doi.org/10.2981/wlb.1995.0030

Cavallini P, Volpi T (1996) Variation in the diet of the red fox in a Mediterranean area. Rev Ecol 51:173–189. https://doi.org/10.2981/wlb.1995.0030

Christiansen P, Wroe S (2007) Bite forces and evolutionary adaptations to feeding ecology in Carnivores. Ecology 88:347–358. https://doi.org/10.1890/0012-9658(2007)88[347:BFAEAT]2.0.CO;2

Churcher CS (1959) The specific status of the New World red fox. J Mammal 40:513–520

Cignoni P, Callieri M, Corsini M, et al (2008) MeshLab: an open-source mesh processing tool. Computing

Cornette R, Herrel A, Cosson J-F, et al (2012) Rapid morpho-functional changes among insular populations of the greater white-toothed shrew. Biol J Linn Soc 107:322–331. https://doi.org/10.1111/j.1095-8312.2012.01934.x

Cox GW (2004) Alien species and evolution: the evolutionary ecology of exotic plants, animals, microbes, and interacting native species. Island Press, Washington DC

Cupples JB, Crowther MS, Story G, Letnic M (2011) Dietary overlap and prey selectivity among sympatric carnivores: could dingoes suppress foxes through competition for prey? J Mammal 590–600. https://doi.org/10.1644/10-MAMM-A-164.1

Davis JL, Santana SE, Dumont ER, Grosse IR (2010) Predicting bite force in mammals: two-dimensional versus three-dimensional lever models. J Exp Biol 213:1844–1851. https://doi.org/10.1242/jeb.041129

Díaz-Ruiz F, Delibes-Mateos M, García-Moreno JL, María López-Martín J, Ferreira C, Ferreras P (2013) Biogeographical patterns in the diet of an opportunistic predator: the red fox Vulpes vulpes in the Iberian Peninsula. Mamm Rev 43:59–70

Dickman CR (1996) Impact of exotic generalist predators on the native fauna of Australia. Wildl Biol 2:185–195. https://doi.org/10.2981/wlb.1996.018

Doherty TS, Davis NE, Dickman CR, et al (2019) Continental patterns in the diet of a top predator: Australia's dingo. Mammal Rev 49:31–44. https://doi.org/10.1111/mam.12139

Doherty TS, Davis RA, van Etten EJB, et al (2015) A continental-scale analysis of feral cat diet in Australia. J Biogeogr 42:964–975. https://doi.org/10.1111/jbi.12469

Dryden IL, Mardia KV (2016) Statistical Shape Analysis With Applications in R. John Wiley & Sons

Edwards CJ, Soulsbury CD, Statham MJ, et al (2012) Temporal genetic variation of the red fox, *Vulpes vulpes*, across western Europe and the British Isles. Quat Sci Rev 57:95–104. https://doi.org/10.1016/j.quascirev.2012.10.010

Fischer DT, Still CJ (2007) Evaluating patterns of fog water deposition and isotopic composition on the California Channel Islands. Water Resour Res 43:4

Fleming P, Corbett L, Harden B, Thomson P (2001) Managing the Impact of Dingoes and Other Wild Dogs. Bureau of Rural Sciences, Canberra

Fleming PA, Crawford HM, Auckland CH, Calver MC (2020) Body size and bite force of stray and feral cats—are bigger or older cats taking the largest or more difficult-to-handle prey? Animals 10(4):707. https://doi.org/10.3390/ani10040707

Fleming PA, Crawford HM, Stobo-Wilson AM, et al (2021) Diet of the introduced red fox *Vulpes vulpes* in Australia: analysis of temporal and spatial patterns. Mammal Rev 51:508–527. https://doi.org/10.1111/mam.12251

Foote M (1993) Contributions of Individual Taxa to Overall Morphological Disparity. Paleobiology 19:403–419

Forbes-Harper JL, Crawford HM, Dundas SJ, et al (2017) Diet and bite force in red foxes: ontogenetic and sex differences in an invasive carnivore. J Zool 303:54–63. https://doi.org/10.1111/jzo.12463

Forsyth T (2004) Critical political ecology: the politics of environmental science. Routledge, New York

Funk WC, Lovich RE, Hohenlohe PA, et al (2016) Adaptive divergence despite strong genetic drift: genomic analysis of the evolutionary mechanisms causing genetic differentiation in the island fox (*Urocyon littoralis*). Mol Ecol 25:2176–2194. https://doi.org/10.1111/mec.13605

Gortázar C, Travaini A, Delibes M (2000) Habitat-related microgeographic body size variation in two Mediterranean populations of red fox (*Vulpes vulpes*). J Zool 250:335–338

Gunz P, Mitteroecker P, Bookstein FL (2005) Semilandmarks in Three Dimensions. In: Slice DE (ed) Modern Morphometrics in Physical Anthropology. Springer US, Boston, MA, pp 73–98

Hand DJ, Taylor CC (1987) Multivariate analysis of variance and repeated measures: A practical approach for behavioural scientists. Chapman & Hall/CRC, Boca Raton, FL

Haxton HA (1944) Absolute muscle force in the ankle flexors of man. J Physiol 103:267–273

Herzog W (1994) Muscle. In: B.M. Nigg, W. Herzog (eds) Biomechanics of the Musculoskeletal System. Wiley, New York, pp 154–187

Holsinger KE, Weir BS (2009) Genetics in geographically structured populations: defining, estimating and interpreting FST. Nat Rev Genet 10:639–650. https://doi.org/10.1038/nrg2611

Hradsky BA, Robley A, Alexander R, et al (2017) Human-modified habitats facilitate forest-dwelling populations of an invasive predator, *Vulpes vulpes*. Sci Rep 7:12291. https://doi.org/10.1038/s41598-017-12464-7

Huson LW, Page RJC (1980) Multivariate geographical variation of the Red fox (*Vulpes vulpes*) in Wales. J Zool 191:453–459. https://doi.org/10.1111/j.1469-7998.1980.tb01477.x

Jojić V, Porobić J, Ćirović D (2017) Cranial variability of the Serbian red fox. Zool Anz 267:41–48. https://doi.org/10.1016/j.jcz.2017.02.001

Kamler J, Ballard W (2002) A review of native and non-native red foxes in North America. Wildl Soc Bull 30:370–379. https://doi.org/10.2307/3784493

Klingenberg CP, Barluenga M, Meyer A (2002) Shape analysis of symmetric structures: quantifying variation among individuals and

asymmetry. Evolution 56:1909–1920. https://doi.org/10.1111/j.0014-3820.2002.tb00117.x
Klingenberg CP, Monteiro LR (2005) Distances and directions in multidimensional shape spaces: implications for morphometric applications. Syst Biol 54:678–688. https://doi.org/10.1080/10635150590947258
Kouvari M, Herrel A, Cornette R (2021) Humans and climate as possible drivers of the morphology and function of the mandible of *Suncus etruscus* in Corsica. J Archaeol Sci 132:105434. https://doi.org/10.1016/j.jas.2021.105434
Krzanowski WJ (ed) (1988) Principles of Multivariate Analysis: A User's Perspective. Oxford University Press, Inc., New York, NY, USA
Lade JA, Murray ND, Marks CA, Robinson NA (1996) Microsatellite differentiation between Phillip Island and mainland Australian populations of the red fox *Vulpes vulpes*. Mol Ecol 5:81–87. https://doi.org/10.1111/j.1365-294X.1996.tb00293.x
Lande R (1979) Quantitative genetic analysis of multivariate evolution, applied to brain: body size allometry. Evolution 33:402–416. https://doi.org/10.1111/j.1558-5646.1979.tb04694.x
Le Maître A, Mitteroecker P (2019) Multivariate comparison of variance in R. Methods Ecol Evol 10:1380–1392. https://doi.org/10.1111/2041-210X.13253
Lewis-Stempel J (2020) The Wild Life of the Fox. Random House
Magalhães AR, Damasceno EM, Astúa D (2020) Bite force sexual dimorphism in Canidae (Mammalia: Carnivora): relations between diet, sociality and bite force intersexual differences. Hystrix Ital J Mammal 31:99–104. https://doi.org/10.4404/hystrix-00332-2020
Martin G, Chapuis E, Goudet J (2008) Multivariate Qst–Fst comparisons: a neutrality test for the evolution of the G matrix in structured populations. Genetics 180:2135–2149. https://doi.org/10.1534/genetics.107.080820
Martin ML, Travouillon KJ, Fleming PA, Warburton NM (2020) Review of the methods used for calculating physiological cross-sectional area (PCSA) for ecological questions. J Morphol 281:778–789. https://doi.org/10.1002/jmor.21139
Mendez J, Keys A (1960) Density and composition of mammalian muscle. Metabolism 9:184–188
Meyer N, Maumy M, Bertrand F (2010) Comparaison de variantes de régressions logistiques PLS et de régression PLS sur variables qualitatives : application aux données d'allélotypage. J Soc Fr Stat 151:1–18
Mitteroecker P, Gunz P, Bernhard M, et al (2004) Comparison of cranial ontogenetic trajectories among great apes and humans. J Hum Evol 46:679–698. https://doi.org/10.1016/j.jhevol.2004.03.006
Newsome, A.E. & Coman, B.J. (1989) Canidae. In: Fauna of Australia 1B: 993–1005. Australian Government Publishing Service, Canberra
Nogueira MR, Peracchi AL, Monteiro LR (2009) Morphological correlates of bite force and diet in the skull and mandible of phyllostomid bats. Funct Ecol 23:715–723. https://doi.org/10.1111/j.1365-2435.2009.01549.x
Parsons KJ, Rigg A, Conith AJ, et al (2020) Skull morphology diverges between urban and rural populations of red foxes mirroring patterns of domestication and macroevolution. Proc R Soc B Biol Sci 287:20200763. https://doi.org/10.1098/rspb.2020.0763
Penrose F, Cox P, Kemp G, Jeffery N (2020) Functional morphology of the jaw adductor muscles in the Canidae. Anat Rec 303:2878–2903: https://doi.org/10.1002/ar.24391
Robley AJ, Reddiex B, Arthur AD, et al (2004) Interactions Between Feral Cats, Foxes, Native Carnivores, and Rabbits in Australia, Commonwealth of Australia
Rohlf F, Slice D (1990) Extensions of the Procrustes method for the optimal superimposition of landmarks. Syst Zool 39:40–59. https://doi.org/10.2307/2992207
Rohlf FJ, Corti M (2000) Use of two-block partial least-squares to study covariation in shape. Syst Biol 49:740–753. https://doi.org/10.1080/106351500750049806
Rolls EC (1969) They All Ran Wild. Angus and Robertson, Sydney
Roulichova J, Andera M (2007) Simple method of age determination in red fox, *Vulpes vulpes*. Folia Zool 56:440
Sacks BN, Statham MJ, Perrine JD, et al (2010) North American montane red foxes: expansion, fragmentation, and the origin of the Sacramento Valley red fox. Conserv Genet 11:1523–1539. https://doi.org/10.1007/s10592-010-0053-4
Saunders G, Coman B, Kinnear J, Braysher M (1995) Managing vertebrate pests: foxes. Australian Government Publishing Service, Canberra
Saunders GR, Gentle MN, Dickman CR (2010) The impacts and management of foxes *Vulpes vulpes* in Australia. Mammal Rev 40:181–211. https://doi.org/10.1111/j.1365-2907.2010.00159.x
Schipper J, Chanson JS, Chiozza F, et al (2008) The status of the world's land and marine mammals: diversity, threat, and knowledge. Science 322:225–230. https://doi.org/10.1126/science.1165115
Schlager S (2013) Soft-tissue reconstruction of the human nose: population differences and sexual dimorphism. Dissertation, Universitätsbibliothek Freiburg, Freiburg
Sih A, Bolnick DI, Luttbeg B, et al (2010) Predator-prey naïveté, antipredator behavior, and the ecology of predator invasions. Oikos 119:610–621. https://doi.org/10.1111/j.1600-0706.2009.18039.x
Sillero-Zubiri C, Hoffmann M, Macdonald DW (2004) Canids: Foxes, Wolves, Jackals, and Dogs: Status Survey and Conservation Action Plan. IUCN Gland, Switzerland
Soe E, Davison J, Süld K, Valdmann H, Laurimaa L, Saarma U (2017) Europe-wide biogeographical patterns in the diet of an ecologically and epidemiologically important mesopredator, the red fox Vulpes vulpes: a quantitative review. Mamm Rev 47:198–211
Spalding MD, Fox HE, Allen GR, et al (2007) Marine ecoregions of the world: a bioregionalization of coastal and shelf areas. BioScience 57:573–583
Statham MJ, Murdoch J, Janecka J, et al (2014) Range-wide multilocus phylogeography of the red fox reveals ancient continental divergence, minimal genomic exchange and distinct demographic histories. Mol Ecol 23:4813–4830. https://doi.org/10.1111/mec.12898
Stepkovitch B, Martin JM, Dickman CR, Welbergen JA (2019) Urban lifestyle supports larger red foxes in Australia: an investigation into the morphology of an invasive predator. J Zool 309:287–294. https://doi.org/10.1111/jzo.12723
Szuma E (2008) Evolutionary and climatic factors affecting tooth size in the red fox *Vulpes vulpes* in the Holarctic. Mammal Res 53:289–332. https://doi.org/10.1007/BF03195193
West-Eberhard MJ (1989) Phenotypic plasticity and the origins of diversity. Annu Rev Ecol Syst 20:249–278
Wiley DF, Amenta N, Alcantara DA, et al (2005) Evolutionary morphing. In: VIS 05. IEEE Visualization, 2005. pp 431–438
Zelditch ML, Swiderski DL, Sheets HD (2012) Geometric Morphometrics for Biologists: A Primer. Academic Press, London